Decay phase aerosol dynamics of an indoor aerosol particle source has a significant role in exposure analysis

Kuisma Vesisenaho¹, Heino Kuuluvainen¹, Ukko-Ville Mäkinen¹, Miska Olin², and Panu Karjalainen¹ Aerosol Physics Laboratory, Faculty of Engineering and Natural Sciences, Tampere University, Tampere, 33014, Finland

²Department of Atmospheric Sciences, Texas A&M University, College Station, TX, USA

Correspondence: Kuisma Vesisenaho (kuisma.vesisenaho@tuni.fi)

Abstract. Indoor particle sources have been recognized as major contributors to aerosol particle exposure posing a health risk particularly to people spending much of their time indoors. Previously, most of the studies examining indoor particle sources have been focusing on active periods of the sources instead of the decay phase of the emitted particle concentration. This gives motivation for this study to investigate the decay of particle lung-deposited surface area (LDSA) concentrations following indoor particle emissions, with a focus on cooking activities. Two decay functions were derived to describe these processes. The first function considers ventilation, particle deposition onto surfaces and a stable background particle source, whereas the second function also includes coagulation. These functions were validated using measurements that covered four dwellings equipped with mechanical ventilation systems. Both decay functions accurately fit the measured data, with the more comprehensive function, including coagulation, consistently achieving lower fitting errors, particularly at high LDSA concentrations. Using urban air quality data of LDSA concentrations from the city of Tampere, the decay functions were further applied to estimate the contribution of cooking to the daily LDSA dose. The cooking-related fraction of exposure dose fraction varied widely, from 17.2 % to 93.9 %, reflecting the influence of cooking styles and ventilation systems. Crucially, from 66.5 to 80.3 % of the cooking-related LDSA dose, using the simpler decay function, and from 72.9 to 82.9 %, using the coagulation-inclusive function, occurred during the decay phase after active cooking. The findings highlight the importance of considering the post-cooking decay phase in total exposure assessments and demonstrate the utility of these functions for interpolating or extrapolating LDSA data. The decay functions derived in this study can be applied to describe other indoor particle sources, distinguish emissions of successive indoor emission events and investigate factors affecting the decay process, such as ventilation.

1 Introduction

Exposure to aerosol particles can cause various negative health effects, such as cardiovascular diseases, diabetes, chronic respiratory diseases, and premature mortality (Kim et al., 2015; WHO, 2021). Especially fine particulate matter (PM_{2.5}), consisting of particles smaller than 2.5 μm, has been strongly linked to the negative health effects of aerosol particles (Liu et al., 2017; Chen and Hoek, 2020). Globally PM_{2.5} is estimated to cause 4.2 (Cohen et al., 2017), 8.9 (Burnett et al., 2018), or 10.2 million (Vohra et al., 2021) premature deaths annually. To prevent the negative health effects, particle concentrations are currently

regulated the exposure to particles resulting from spending time at elevated particle concentrations should be reduced. One approach, currently adopted, is to regulate particle concentrations by guidelines (WHO, 2021) and legislation (EU, 2008; EPA, 2013). For instance, in the European Union, the reduction of PM_{2.5} concentration achieved by legislation and technology measures between 1970 and 2010 is estimated to have resulted in an annual financial benefit of 232 billion US dollars (Turnock et al., 2016).

30

35

However, the regulations and monitoring of particle concentrations mainly focus on outdoor air quality, although people living in developed countries spend approximately from 80 to 95 percent of their time indoors (Hussein et al., 2012; Yoon et al., 2022; EPA, 2011). Scungio et al. (2020) have proposed based on their study conducted in Italy, that exposure to particles that the particle dose could be underestimated by 35 percent if the dose is determined by if assessed using city-scale outdoor particle concentrations measured at the city scale rather than on a personal scale including, rather than personal-scale measurements that account for both indoor and outdoor exposure. This underestimation could further increase as outdoor air quality improves. The finding of Scungio et al. (2020) highlights the importance of measuring indoor aerosol even though the variance of indoor particle concentrations in time and between different spaces is greater than that of outdoors making it more challenging to measure.

Indoor particle sources are typically related to burning or thermal processes and because of that cooking, smoking, candle burning and the usage of electrical devices are considered as the main sources of indoor particles (Hussein et al., 2006; Wallace and Ott, 2011; Isaxon et al., 2015; Zhao et al., 2021). It has been estimated that indoor sources contribute 56 % of the daily exposure to particle number particle number dose in developed countries (Zhao et al., 2021). Often, the sources are active only for short periods, but, for example, decay of the high cooking-generated particle concentration can take from an hour to several hours (Hussein et al., 2006; Wan et al., 2011; Isaxon et al., 2015). Due to the long decay time, it has been suggested observed that cooking-generated particles eould can induce significant exposure after the cooking action, for instance, during a night's sleep (Pacitto et al., 2018). (Pacitto et al., 2018; Zhao et al., 2021). Pacitto et al. (2021) have reported that the contribution of cooking and eating activities to the daily particle dose varies from 13 to 59 % in western cities and from 7 to 14 % in cities located in low- and middle-income countries. The same study also shows that, in general, women are receiving higher doses of cooking-generated particles. Additionally, it has been shown that the particle dose received from cooking varies greatly depending on ventilation style, ingredients, cooking style and stove type (Kang et al., 2019; Abdullahi et al., 2013; Wallace and Ott, 2011)

Morawska et al. (2013) have estimated, based on measurements carried out by Wallace and Ott (2011), that cooking produces 47 % of ultrafine particles (UFPs) indoorswhile indoor UFPs are. Moreover, indoor UFPs have been estimated to cause 67 (Wallace and Ott, 2011), 59 (Bhangar et al., 2011), or 31 (Mullen et al., 2011) percent % of the total exposure to dose of UFPs. Ultrafine particles having a diameter of 100 nm or below have been concerned as a health risk (WHO, 2021) due to their ability to enter the bloodstream via lungs (Nemmar et al., 2002; Ohlwein et al., 2019). Through the circulatory system a small fraction of UFPs can deposit in distal organs, including the heart, kidneys, and the liver (Oberdörster et al., 2005; Schraufnagel, 2020). Additionally, UFPs have been found to translocate to the brain via the olfactory nerve (Oberdörster et al., 2004) (Oberdörster et al., 2004; Kanninen et al., 2020). Studies also suggest that UFPs have higher toxicity per mass unit, in compar-

ison to larger particles, likely as a result of a greater surface area that leads to a higher oxidative potential (Donaldson et al., 2002; Monteiller et al., 2007).

When assessing exposure to aerosol particles, it is highly important that the quantity describing particle concentration correlates well with the health effects. However, the negative health responses to PM_{2.5} mass concentration, the most commonly used particle concentration quantity in the current regulations, vary between different cities or regions (Li et al., 2019). Therefore, in this study, particle concentration is described by lung deposited surface area (LDSA) concentration that combines the surface area concentration of particles and the deposition efficiency of particles into the human respiratory tract. According to Schmid and Stoeger (2016) this combination makes LDSA concentration, from the toxicological perspective, the most relevant concentration metric to indicate the negative health effects of particles. Lepistö et al. (2023) and Salo et al. (2021) have also found that using LDSA when LDSA is used as a metric instead of PM_{2.53} the differences in the strength of the health response to particles narrow between different geographical regions become narrower. In addition to the ability of describing health effects, LDSA concentration is relatively easy and inexpensive to measure with sensor type instruments when the particle size is between 20 and 400 nm (Todea et al., 2017; Fierz et al., 2011, 2014). This size range is suitable for measuring the majority of particles emitted from indoor sources such as cooking (Wallace, 2006; Buonanno et al., 2009; Wan et al., 2011; Abdullahi et al., 2013). However, the downside of choosing LDSA concentration as particle concentration unit is that there are no already solved decay functions for the decay process of LDSA concentration.

Exposure to particles emitted from indoor sources is highly connected to the characteristics of indoor environments and ventilation. Finland is an example of a country in which the mechanical supply and exhaust ventilation with supply air filtration and heat recovery is required in new buildings since 2003 (Hänninen et al., 2005). According to the National Building Code of Finland (section D2, 2003), the air exchange rate should be 0.35 dm³s⁻¹m⁻² that, in 2.5 m high space, corresponds to a ventilation rate of 0.5 h⁻¹, which has been the standard also in many other countries in Europe (Dimitroulopoulou, 2012). A recent study by Zukowska et al. (2021) showed that mechanical ventilation is becoming a common choice in several European countries induced by the need to reduce the energy consumption of buildings. In developing countries, natural ventilation still dominates in residential buildings, but global mega-trends, such as climate change and urbanization, will evidently increase the need for air conditioning and air infiltration for which the mechanical ventilation is beneficial (Ahmed et al., 2021; Niculita-Hirzel, 2022). While mechanical ventilation reduces the exposure to outdoor particles (Park et al., 2014; Silvonen et al., 2023), buildings equipped with mechanical ventilation are usually airtight which slows down the decay process of indoor generated particles. This emphasizes offers one explanation, why cooking related LDSA exposure has more significance in developed countries, considered in this study, as Pacitto et al. (2021) report. Altogether, these findings emphasize the need for characterization of aerosol dynamics of the decay phase in mechanical ventilated dwellings.

The aim of this study is to first develop aerosol dynamics—based decay functions describing the decay phase of indoor particle emission using LDSA concentration as the metric. Subsequently, the second objective is to investigate the impact of cooking, including the decay phase of cooking-generated particles, on the daily LDSA exposure dose applying the decay functions. The experiments are carried out using sensor type devices to measure LDSA concentration in four different dwellings equipped with mechanical ventilation system.

95 2 Decay functions

100

105

120

125

Indoor particle sources are often active for only a short period of time, yet they produce high particle concentrations which decay slowly in an indoor environment (Hussein et al., 2006; Wan et al., 2011; Isaxon et al., 2015). As a result, a measurement covering only the active time of the particle source is not enough to asses the total source-induced exposure. A decay function describing the decay phase of the particle concentration resulted from the source would provide a useful tool for extending the observation outside of the measured time period and for further understanding the dilution process. In addition, the decay function could be applied to distinguish the emissions of successive emission events from one another. In this study, two decay functions are derived from the solutions of differential equations. The first function considers ventilation and particle deposition onto walls, which are the most essential aerosol processes indoors (Nazaroff, 2004). The second decay function also includes coagulation, which becomes a relevant process with high particle concentrations. Furthermore, both decay functions consider a stable background source that covers, for example, particles transferred from outdoor air.

2.1 Decay function considering ventilation and deposition

Ventilation can be categorized to mechanical, natural, and leakage ventilation that accounts for aerosol flow through cracks in the building's envelope (Nazaroff, 2004). All of these ventilation processes can be present at the same time, for instance, when a window is opened in a mechanical ventilated dwelling. In mechanical ventilation, supply air is filtered with the efficiency $\eta_{\rm M}$, and in leakage ventilation the size and the shape of the cracks determines the penetration factor P denoting the fraction of particles transferring from outdoor to indoor air. Both, the filter efficiency and the penetration factor, depend on the particle size. Using this classification and assuming that the indoor air is well-mixed, the ventilation-related time behaviour of LDSA concentration can be described by differential equation

$$\frac{\mathrm{d}C_{\mathrm{LDSA,i}}}{\mathrm{d}t}\frac{\mathrm{d}C_{\mathrm{LDSA,i,v}}}{\mathrm{d}t} = C_{\mathrm{LDSA,o}}\frac{(1-\eta_{\mathrm{M}})Q_{\mathrm{M,in}} + Q_{\mathrm{N,in}} + Q_{\mathrm{L,in}}P}{V} - C_{\mathrm{LDSA,i}}\frac{Q_{\mathrm{M,out}} + Q_{\mathrm{N,out}} + Q_{\mathrm{L,out}}P}{V},\tag{1}$$

where V is the volume of the indoor space and $Q_{\rm M}$, $Q_{\rm N}$, and $Q_{\rm L}$ are the flow rates of mechanical, natural and leakage ventilation, respectively. The additional subscript of the flow rates also indicates the direction of the flow. Indoor LDSA concentration $C_{\rm LDSA,i}$ and outdoor LDSA concentration $C_{\rm LDSA,o}$ are defined as

$$C_{\rm LDSA} = \int \frac{\mathrm{d}C_N}{\mathrm{d}d_{\rm p}} A_{\rm p} \mathrm{DF}_{\rm al} \, \mathrm{d}d_{\rm p},\tag{2}$$

where C_N is the particle number concentration, d_p is the particle diameter, A_p is the surface area of a particle, and DF_{al} is the size dependent deposition fraction of particles to alveolar region of the human lungs. Looking at the right side of Eq. (1), the first term represents the supply ventilation transporting LDSA concentration from outdoor to indoor air and the second term stands for the exhaust ventilation transporting LDSA concentration in the opposite direction.

In addition to ventilation, deposition to the surfaces of the indoor space has an effect on the indoor LDSA concentration. According to Nazaroff (2004), diffusion and gravitational settling are the main deposition mechanisms indoors depending on the particle size. By converting the differential equation for mass concentration presented by Nazaroff and Cass (1989) to

LDSA concentration, the decrease in LDSA concentration driven by deposition can be expressed as

$$\frac{\mathrm{d}C_{\mathrm{LDSA,i}}}{\mathrm{d}t}\frac{\mathrm{d}C_{\mathrm{LDSA,i,de}}}{\mathrm{d}t} = -C_{\mathrm{LDSA,i}}\frac{\sum_{j}v_{d_{\mathrm{p}},\mathrm{LDSA},j}A_{j}}{V},\tag{3}$$

where the index j spans the surfaces of the indoor space so that A_j is the area of a surface and $v_{d_p, \text{LDSA}, j}$ is the mean deposition velocity of LDSA. Using the particle size dependent deposition coefficient of LDSA β_{LDSA} , Eq. (3) can be simplified to

130
$$\frac{\mathrm{d}C_{\mathrm{LDSA,i}}}{\mathrm{d}t} \frac{\mathrm{d}C_{\mathrm{LDSA,i,de}}}{\mathrm{d}t} = -\beta_{\mathrm{LDSA}}C_{\mathrm{LDSA,i}}.$$
 (4)

It has to be noted that the values of $\beta_{\rm LDSA}$ differ from more commonly used deposition coefficients of particle number or mass (Crump et al., 1982; Lai, 2002). This difference can be understood from Eq. (3) where the deposition velocity is for LDSA instead of mass or number. However, from the same equation, it can be seen that the deposition coefficient depends on the geometry of the studied indoor space, in which case the comparison of deposition coefficients is not useful even when the metrics of particle concentration would match.

By combining Eq. (1) and Eq. (4) and including the supply ventilation term of Eq. (1) to the constant background source $S_{\rm LDSA}$ assuming that outdoor LDSA concentration stays constant, the time behaviour of indoor LDSA concentration can be described as a differential equation

$$\frac{\mathrm{d}C_{\mathrm{LDSA,i}}}{\mathrm{d}t} = -C_{\mathrm{LDSA,i}} \frac{Q_{\mathrm{M}} + Q_{\mathrm{N}} + Q_{\mathrm{L}} P}{V} - \beta_{\mathrm{LDSA}} C_{\mathrm{LDSA,i}} + S_{\mathrm{LDSA}}.$$
 (5)

Because the first and the second term of the right side of Eq. (5) are both first-order they can be further combined using the dilution coefficient $D_{\rm LDSA}$ so that the differential equation is written

$$\frac{\mathrm{d}C_{\mathrm{LDSA,i}}}{\mathrm{d}t} = -D_{\mathrm{LDSA}}C_{\mathrm{LDSA,i}} + S_{\mathrm{LDSA}}.\tag{6}$$

The solution of Eq. (6) is a time-dependent function for indoor LDSA concentration

135

$$C_{\rm LDSA,i} = e^{-D_{\rm LDSA}t} \left(C_{\rm LDSA,i,0} - \frac{S_{\rm LDSA}}{D_{\rm LDSA}} \right) + \frac{S_{\rm LDSA}}{D_{\rm LDSA}},\tag{7}$$

where $C_{\rm LDSA,i,0}$ is the initial indoor LDSA concentration at the start of the decay process. Looking at Eq. (6)-(7) as time approaches infinity, the time derivative of LDSA concentration approaches zero and LDSA concentration approaches background concentration $C_{\rm LDSA,i,bg}$ resulted from the background source. Consequently, as time approaches infinity, Eq. (6) can be stated as $S_{\rm LDSA} = D_{\rm LDSA}C_{\rm LDSA,i,bg}$. Substituting this into Eq. (7), the equation can be formulated into form

$$C_{\text{LDSA,i}} = C_{\text{LDSA,i,bg}} + (C_{\text{LDSA,i,0}} - C_{\text{LDSA,i,bg}})e^{-D_{\text{LDSA}}t}, \tag{8}$$

50 where the initial and the background indoor LDSA concentrations can be measured making the dilution coefficient the only fitting parameter. In Supplement S1.1, the equation is derived in more detail starting from Eq. (6). Equation (8) is estimated to be functional in indoor emission events with particle number concentrations under 10^4 cm⁻³ leading to a negligible role of coagulation (Hussein et al., 2009).

2.2 Decay function considering ventilation, deposition, and coagulation

165

However, if the indoor particle concentration rises higher than 10⁴ cm⁻³, which is typical, for example, as a result of cooking (Wallace, 2006; Buonanno et al., 2009; Pacitto et al., 2018), coagulation starts to act as a notable aerosol process that has an effect on the time behaviour of indoor particle concentration. Modeling Modelling the coagulation of an aerosol consisting of several size modes is feasible, but it leads to a relatively complicated form of equations (Whitby and McMurry, 1997). Therefore, in this study straightforward assumptions, that all particles of the studied aerosol are equal in size and the coagulation coefficient stays constant as a function of time, are applied. With these assumptions, the effect of coagulation on particle number concentration can be described using a differential equation

$$\frac{\mathrm{d}C_N}{\mathrm{d}t} \frac{\mathrm{d}C_{N,\mathrm{cg}}}{\mathrm{d}t} = -\frac{1}{2}KC_N^2,\tag{9}$$

where K is the coagulation coefficient and the factor -1/2 consists of multiplication of 1/2, by which calculation of one collision as two collisions between same particles is avoided, and -1, that is the change of particle number when two particles collide and adhere forming larger particle. To convert Eq. (9) from particle number to LDSA, the change of LDSA, when two particles of same size coagulate forming a larger particle, has to be evaluated. This change, $\Delta LDSA$, can be expressed as

$$\Delta LDSA = \left[\left(N_{d_{p,1}} - 2 \right) A_{p,d_{p,1}} DF_{al,d_{p,1}} + A_{p,d_{p,2}} DF_{al,d_{p,2}} \right] - N_{d_{p,1}} A_{p,d_{p,1}} DF_{al,d_{p,1}}, \tag{10}$$

where $N_{d_{p,1}}$, $A_{p,d_{p,1}}$, and $DF_{al,d_{p,1}}$ are the number, the surface area, and the alveolar deposition efficiency of the initial particles with the size of $d_{p,1}$, respectively. Correspondingly, $A_{p,d_{p,2}}$ and $DF_{al,d_{p,2}}$ are the surface area and the alveolar deposition efficiency of the formed particle with the size of $d_{p,2}$, respectively. In Eq. (10), the expression inside brackets accounts for the final state, in which two initial particles have transformed to one larger particle, and the last term represents the initial state.

To further investigate the change of LDSA in coagulation, the alveolar deposition efficiency and the particle surface area have to be expressed as a function of the particle size. The alveolar deposition efficiency can be estimated using the human respiratory tract model of ICRP (1994). In the size range of 30 to 300 nm, the model can be parameterized at a reasonable accuracy with using the expression DF_{al} $\approx ad_p^{-1}$, where a is 14.37 nm. Whereas, by The coefficient of determination (R²) for the parametrization is 0.987. By assuming that the particles are spherical, the surface area can be simply expressed as $A_p = \pi d_p^2$. Substituting this expression to Eq. (10), the equation can be rearranged into form

$$\Delta LDSA \approx \pi d_{p,2}^2 a d_{p,2}^{-1} - 2\pi d_{p,1}^2 a d_{p,1}^{-1}.$$
(11)

When mass is conserved and the density of spherical particles is assumed to be equal between the initial and the formed particles, a relation between the initial particle size and the size of the formed particle is

$$\frac{1}{6}\rho\pi d_{\mathbf{p},1}^3 + \frac{1}{6}\rho\pi d_{\mathbf{p},1}^3 = \frac{1}{6}\rho\pi d_{\mathbf{p},2}^3,\tag{12}$$

where ρ is the density of a particle. By solving Eq. (12), the size of the formed particle can be expressed with respect to the initial particle size as $d_{p,2} = 2^{1/3} d_{p,1}$. Substituting this expression into Eq. (11) gives

$$\Delta LDSA \approx 2\pi a \left(2^{-\frac{2}{3}} - 1\right) d_{p,1}. \tag{13}$$

Another equation that is needed for converting Eq. (9) for LDSA concentration is the relationship between number concentration and LDSA concentration. In the case of particles of only one size and using expressions $DF_{al} \approx ad_p^{-1}$ and $A_p = \pi d_p^2$, this relationship can be solved from Eq. (2) into form

$$C_N \approx \frac{1}{\pi a} C_{\text{LDSA}} d_p^{-1}.$$
 (14)

Finally, substituting the factor -1 with Eq. (13) and the number concentration with Eq. (14), Eq. (9) can be transformed to describe the effect of coagulation on LDSA concentration as

$$\frac{\mathrm{d}C_{\mathrm{LDSA}}}{\mathrm{d}t}\frac{\mathrm{d}C_{\mathrm{LDSA,cg}}}{\mathrm{d}t} = \frac{1}{\pi a} \left(2^{-\frac{2}{3}} - 1\right) d_{\mathrm{p}}^{-1} K C_{\mathrm{LDSA}}^{2},\tag{15}$$

where coagulation coefficient is the same as in Eq. (9). Equation (15) can be simplified to

$$\frac{\mathrm{d}C_{\mathrm{LDSA}}}{\mathrm{d}t}\frac{\mathrm{d}C_{\mathrm{LDSA,cg}}}{\mathrm{d}t} = -K_{\mathrm{LDSA}}C_{\mathrm{LDSA}}^{2},\tag{16}$$

where $K_{\rm LDSA}$ is the coagulation coefficient for LDSA, which is

195
$$K_{\text{LDSA}} = -\frac{1}{\pi a} \left(2^{-\frac{2}{3}} - 1 \right) d_{\text{p}}^{-1} K.$$
 (17)

When Eq. (16) is applied to indoor LDSA concentration and combined with Eq. (6), time behaviour of indoor LDSA concentration driven by ventilation, deposition onto surfaces and coagulation is described as a differential equation

$$\frac{\mathrm{d}C_{\mathrm{LDSA,i}}}{\mathrm{d}t} = -D_{\mathrm{LDSA}}C_{\mathrm{LDSA,i}} - K_{\mathrm{LDSA}}C_{\mathrm{LDSA,i}}^2 + S_{\mathrm{LDSA}}.$$
(18)

This second order differential equation has an analytical solution of

200
$$C_{\text{LDSA},i} = \frac{1}{2K_{\text{LDSA}}} \left\{ b - D_{\text{LDSA}} - 2b \left[\left(\frac{2b}{b - D_{\text{LDSA}} - 2K_{\text{LDSA}}C_{\text{LDSA},i,0}} - 1 \right) e^{bt} + 1 \right]^{-1} \right\},$$
 (19)

where an auxiliary variable $b = \sqrt{D_{\rm LDSA}^2 + 4K_{\rm LDSA}S}$ is utilized. Similarly to Eq. (7), the background source term can be expressed using background LDSA concentration. The investigation of Eq. (18) as time approaches infinity gives $S = D_{\rm LDSA}C_{\rm LDSA,i,bg} + K_{\rm LDSA}C_{\rm LDSA,i,bg}^2$. Using this expression, the auxiliary variable b can be written as

$$b = D_{\rm LDSA} + 2K_{\rm LDSA}C_{\rm LDSA,i,bg}.$$
 (20)

Now, Eq. (20) can be applied to transform Eq. (19) to a more simplified form

210

$$C_{\text{LDSA,i}} = C_{\text{LDSA,i,bg}} + b \left[\left(\frac{b}{C_{\text{LDSA,i,0}} - C_{\text{LDSA,i,bg}}} + K_{\text{LDSA}} \right) e^{bt} - K_{\text{LDSA}} \right]^{-1}, \tag{21}$$

where dilution and coagulation coefficients of LDSA, also included in the auxiliary variable b, are the fitting parameters, as initial and background LDSA concentrations can be measured. In Supplement S1.2, the equation is derived in more detail starting from Eq. (18). Comparing Eq. (21) to Eq. (8), the form of the function is more complex and the number of parameters is also by one higher. Because of this, it might be worth to consider, in which cases the presumably more accurate Eq. (21) is reasonable to use instead the simpler Eq. (8).

Table 1. The specification of measurement sites in Cases I to IV.

Case	Building type	Floor area Total floor area (m²)	Cooking space volume (m ³)	Extra ventilation during cooking Building year	Location type
I	Apartment	22	~40	No- 2022	Urban
II	Terraced house	85	~150	Yes 2010	Suburban
III	Terraced house	52.5	~85	Yes 2017	Suburban
IV	Detached house	128.8	~180	Yes -2007	Suburban

Table 2. The specification of cooking measurements in Cases I to IV. Considering extra ventilation during cooking, range hoods were divided into two types. Type 1 range hood has its own exhaust channel, whereas type 2 range hood is connected to the exhaust ventilation system of the dwelling

Case	Date	Cooking start time	Decay end time	Cooking duration (min)	Stove type	Extra ventilation during cooking
Ĭ.	13.9.2022	10:53:28	14:03:07	8.43	Induction	Not used
$\widecheck{\mathbf{II}}_{\sim}$	20.9.2022	10:40:00	13:50:00	9.00	Radiant	Range hood, type 1
$\overline{\mathrm{III}}$	26.9.2022	17:10:12	20:14:22	13.54	Radiant	Range hood, type 2
$\widetilde{\mathbf{IV}}$	13.10.2022	10:32:00	13:37:51	5.85	Induction	Range hood, type 1

3 Experimental methods Methods

3.1 Experiments and measurement devices

To validate the decay functions derived in Sect. 2, measurements investigating indoor particle emissions of cooking in residential buildings were conducted between 13 September 2022 and 13 October 2022. The measurements took place in Tampere region, Finland. With a population of approximately 244 000, Tampere represents an average European city where the population is around 249 000 computed from the most recent population values of European cities provided by Eurostat (2024).

The A total of four measurements, designated as Cases I to IV, took place were conducted in four different dwellings equipped with mechanical supply and exhaust ventilation systems. The measurement sites included one apartment, two terraced houses, and one detached house with floor area ranging from 22 m² to 128.8 m². The dwellings of Cases II to IV are located in a suburban area, whereas the apartment of Case I is located in an urban area, which might have an effect on background particle concentration. The dwellings of the measurement cases are described more precisely in Table 21. In addition, the floor plans are represented case by case in Supplement S2.

In all Cases, the measurement setup consisted of three Partector sensors (Naneos GmbH) measuring LDSA concentration and a DiSCmini sensor measuring geometric mean diameter (GMD), LDSA concentration, and number concentration of particles (Matter Aerosol AG). Both monitors first charge particles using a unipolar diffusion charger followed by the measurement of electric current caused by the charged particles. However, the Partector charges particles periodically and measures the current induced in a Faraday cage (Fierz et al., 2014), while the DiSCmini charges particles continuously and measures current resulting from captured particles in two stages, a diffusion stage and a filter stage (Fierz et al., 2011). In both sensors, LDSA concentration is determined using the fact that, in the size range of 20 to 300 nm, LDSA concentration is approximately directly proportional to the electrical charge of particles resulting in the current. The estimate of the geometric mean diameter provided by the DiSCmini is based on a calibrated particle size distribution and the ratio of currents of the two stages (Fierz et al., 2011).

For the LDSA concentration of the Partector and the number concentration of the DiSCmini, manufactures report a measurement accuracy of ± 30 %. According to Naneos GmbH, for the Partector, this accuracy holds in the particle size range of 20 to 400 nm while the sensor is able to detect particles from 10 nm up to 10 μ m. Whereas, for the DiSCmini, the given accuracy is reported to apply in the whole size range of 20 to 700 nm when the mode of the size distribution is, on a number basis, between 20 and 300 nm. Todea et al. (2017) investigated the accuracy of both sensors, in the accurate size ranges reported by manufacturers, with a large variety of test aerosols by comparing the results to ones measured with a scanning mobility particle sizer (SMPS) or a condensation particle counter (CPC). The study shows that on average the underestimate underestimation of LDSA concentration is 12 and 7 % for the Partector and the DiSCmini, respectively. In addition, the DiSCmini is, on average, observed to overestimate the number concentration by 32 % and underestimate the mean particle size by 10 %. Based on these results, the Partector and the DiSCmini are capable of measuring the LDSA concentration of cooking-generated particles, that are dominated by UFPs in number concentration and typically have the mode of surface area distribution below 400 nm (Buonanno et al., 2009; Wan et al., 2011), with reasonable accuracy for validating the derived decay functions.

In the measurement setups of this study, the first Partector and the DiSCmini were located stationary in the living room, the second Partector was carried around in a backpack sampling aerosol from the breathing zone, and the third Partector was placed stationary outside of the dwelling. An example of the locations of the stationary sensors and the stove is presented in Fig. 1 while all of the setups are presented in Supplement S2. In Cases from II to IV, the sensors located in the living room were placed in the opposite corner from the stove and a meter apart from the walls, but in Case I the placement differed due to furniture and the small size of the apartment. During the cooking, the backpack sensor was close to the stove as the resident wearing the backpack was in charge of the cooking. After the cooking event, the measurement backpack was carried around in different rooms to observe how the particle emissions spread across the dwelling. The outside sensor was placed in a protective bag to keep the temperature of the Partector more stable.

The measurement started with a zero measurement of 5 minutes through a high efficiency particulate air filter (HEPA) followed by 15 minutes long background measurement. In these measurements, all sensors were sampling from the same pipeline. The mean LDSA concentration values of Partectors varied between 0.64 and 1.25 μm^2 cm⁻³ during the zero measurements. Moreover, the differences between Partectors in the average LDSA concentrations of the background measurements were below 1 μm^2 cm⁻³ in all Cases. After making sure that the readings of the sensors were in line, the sensors were placed in their

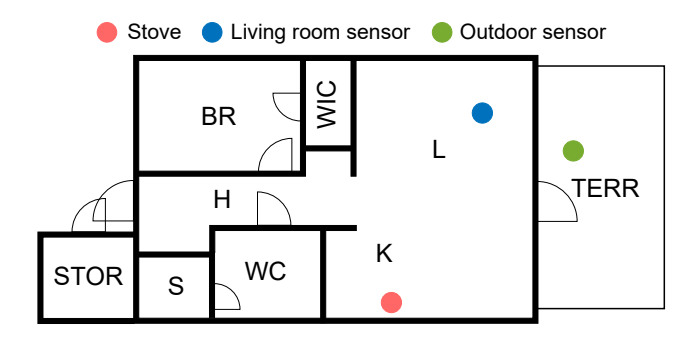


Figure 1. The locations of the stove, the living room sensor, and the outdoor sensor in Case III as an example of the measurement setup in this study. The acronyms of the floor plan are explained in Table S2.1.

locations described above. In those locations, an hour of background was measured before the cooking started. During the cooking, 250 grams of raw chicken strips were pan fried with 15 ml of rapeseed oil. In all Cases, the stove was electricaland, apart, but both induction and ceramic radiant cooktops were included as Table 2 shows. Apart from Case I, ventilation was enhanced during cooking. In Cases II and IV, extra ventilation was achieved using a range hood that has its own exhaust channel, whereas, in Case III the range hood is connected to the exhaust ventilation system of the dwelling. The duration of the cooking event was widely varying probably due to different cooking styles and stove models. The shortest cooking time was 5 min and 51 s, whereas the longest cooking event took 13 min and 33-32 s. Table 2 presents more an accurate description of the measurements in each case. After the cooking, the decay phase of indoor particles was measured for 3 hours, during which the measurement backpack was carried around in different rooms of each dwelling and no extra ventilation or mixing was applied. However, the backpack measurement data were not further utilized in the computation of this study. For that reason, the movement information of the backpack measurement is only presented in the field log of the data publication to enable further analysis (Vesisenaho et al., 2025).

To evaluate the role of cooking-generated particles in the total exposure to aerosol particles, the outdoor LDSA concentrations at two measurement stations in Tampere, Epilä and Pirkankatu, were requested from the city of Tampere. The measurement station of Epilä is located in a suburban area, whereas Pirkankatu is located in an urban area. The data covered one year starting from 1 November 2021 and was measured in both stations with diffusion charging AQ Urban sensors (Pegasor Ab). The sensor is based on the Pegasor PPS-M sensor that measures the net current escaping the instrument due to the outflow of charged particles (Rostedt et al., 2014; Kuula et al., 2019). The correlation between the current of AQ Urban sensor and LDSA concentration measured with a differential mobility particle sizer (DMPS) has been found to be strong ($R^2 = 0.93$) with an error of 19 % in urban air quality measurements conducted by Kuula et al. (2019).

3.2 Algorithm for determining the length of the mixing phase

260

265

270

275

In previous studies investigating the time behaviour of cooking-generated particles indoors, it has been observed that the highest concentration could be reached after the active cooking event (Kim et al., 2018; Tang et al., 2024; Kang et al., 2019).

Additionally, for the minutes following the cooking event, the variation of the concentration has been observed to be higher than on average during the decay process (Kim et al., 2018; Kang et al., 2019). However, the decay functions derived in this study are not able to describe both the increase of concentration resulted from a periodic source and the decay of concentration within one fit. The functions also include assumption that the aerosol is well mixed. Consequently, the observations of the previous studies suggest that it might not be possible to utilize the decay functions immediately after the cooking event.

To solve this challenge, a mixing phase was introduced as a time period that includes both the potential concentration increase and the mixing related variation of concentration. The length of the mixing phase was determined by an algorithm based on the normalized root mean square error (NRMSE) of a fitted decay function following Eq. (21). According to the algorithm, the normalization is performed using the mean value of data points, and the decay function including coagulation is selected for the algorithm because the highest concentrations, where coagulation might have a substantial role, are likely to be measured in the mixing phase. Next, in the algorithm, the decay function is fitted to the time series of LDSA concentration using a non-linear least squares method and with a varying starting point. In the first fit, the starting point is the first measurement point after the cooking event and then it is shifted 5 seconds forward in every fit covering the first 20 minutes following the cooking event. The relative deviation from minimum NRMSE is expected to stabilize near the minimum at a certain time indicating the length of the mixing phase. The starting point of the first fit having NRMSE within 10 % of the minimum NRMSE is defined as the end point of the mixing phase.

3.3 Dose calculation

285

290

295

In this study, the daily LDSA dose received by the population of the Tampere region was assessed by combining the results of cooking measurements, the fits of the decay functions, and the observations of outdoor air quality. The total dose of cooking-generated particles was calculated by summing the background subtracted LDSA doses during the cooking, mixing, and extrapolated decay phases. The decay phase was extrapolated using the fitted decay function and the LDSA doses δ_{LDSA} are determined using equation

$$\delta_{\text{LDSA}} = \text{IR} \int_{t_0}^{t_1} C_{\text{LDSA}} \, dt, \tag{22}$$

where IR is the inhalation rate (IR), while t_0 and t_1 are the start and the end point of the phase, respectively. The daytime IR of $16.3 \, \mathrm{l} \, \mathrm{min}^{-1}$ was computed as the average IR excluding sleep or nap time for individuals aged from 21 to 60 years based on the statistics of EPA (2009). In the case of cooking and mixing phase, the integrand was the LDSA concentration of the living room subtracted by the mean indoor background concentration. The integration is performed numerically using the trapezoidal rule. The dose of the extrapolated decay phase was computed using the integral of the background term subtracted fits of Eq. (8) and Eq. (21). To get the total dose of the extrapolated decay phase, the integral of Eq. (22) was calculated from the starting point of the decay phase to infinity. Despite integrating to infinity, the total dose of a single cooking event was verified to be suitable for assessing a daily dose, because in all Cases the integral increased by less than 1 % after 12 hours of decay.

The outdoor air quality data of Tampere was utilized to estimate the average background doses of indoor and outdoor environments. As the mean LDSA concentrations of day and night, presented in Sect. 4.3, were used to compute the background doses, Eq. (22) could be simplified to form

$$\delta_{\rm LDSA} = \operatorname{IR}\overline{C}_{\rm LDSA}\Delta t,\tag{23}$$

where \overline{C}_{LDSA} is the average LDSA concentration and Δt is the time spent in a certain environment. The estimate for the indoor dose was computed in two parts using Eq. (23). First, the indoor dose during the night was calculated using the nighttime mean concentration of Tampere's air quality stations and I/O-ratio of 0.44, which has been determined by Silvonen et al. (2023) for an office building located in Tampere.

In the calculation of the nightly indoor dose, the length of a night was assumed to be 8 hours and the average sleep or nap IR of 4.8 l min⁻¹ (EPA, 2009) was used. Secondly, the indoor dose during daytime was computed from the daytime mean concentration of Tampere using the I/O-ratio, the daytime IR, and the average time spent indoors in Finland provided by Hussein et al. (2012). The sleep time assumed in this study, 8 hours, was subtracted from the indoor-spent time of 21 hours and 26 minutes.

4 Results and discussion

320

325

330

335

340

4.1 Cooking measurements

In all Cases, cooking was observed to induce one to three orders of magnitude higher LDSA concentrations compared to the background concentrations measured before the cooking event. This is illustrated in Fig. 2, which presents the time series of cooking experiments including the background measurements. The highest concentration was measured in Case I, where the mean concentration during the cooking event was $1800 \, \mu m^2 \, cm^{-3}$ in the living room. Regarding the cooking event and from the perspective of personal exposure, the backpack measurement would be more representative than the living room measurement but in Case I there was an interruption in the backpack measurement during that period. However, due to the small size of the apartment in Case I, the living room measurement was carried out within 3 meters of the stove. In Cases from II to IV, the mean LDSA concentrations of backpack measurement during the cooking event were 9.8, 75.9, and 13.7 $\mu m^2 \, cm^{-3}$, respectively. The difference between the concentration levels of Case I and other Cases is at least partially explained by most probably explained by higher frying pan temperature related to cooking style in Case I and the fact that extra ventilation was not used in Case I. During the cooking event, the 5 minute average of the geometric mean particle size presented in Fig. 2 was within the size range of UFPs in all Cases, which indicates that the cooking emission is in the accurate size range of the Partector. Due to the significant oscillation of the mean particle size in low particle concentrations, the size is presented only when the mean LDSA concentration of 5 minute period is at least 5 μ m² cm⁻³.

Compared to previous studies, the LDSA concentrations of the cooking event are relatively low in Cases from II to IV whereas in Case I the concentration is comparatively high (Geiss et al., 2016; Pacitto et al., 2018; Scungio et al., 2020; Pacitto et al., 2021). For instance, Pacitto et al. (2018) reported the median LDSA concentrations of indoor cooking events in developed

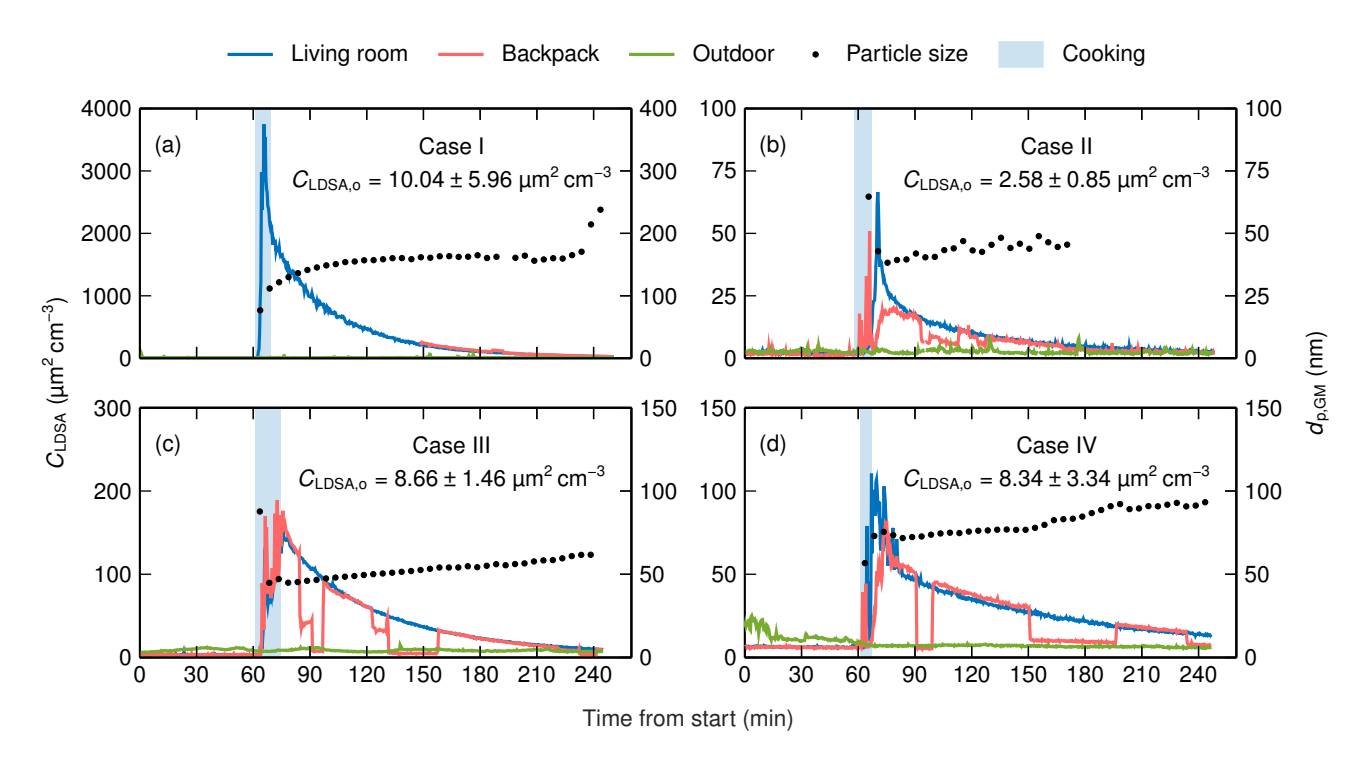


Figure 2. Time series of living room, backpack, and outdoor LDSA concentrations and particle size as GMD in Cases I (a), II (b), III (c), and IV (d). The time series cover the background measurement and the whole cooking experiment including 3 hours of decay. LDSA concentrations are measured using Partectors and mean particle sizes using the DiSCmini. The mean particle size is presented as a 5 minute average when LDSA concentration is at least 5 μ m² cm⁻³. In addition, the mean and the standard deviation of outdoor LDSA concentration are presented numerically.

countries. In that study, the highest median concentration of $1362 \, \mu m^2 \, cm^{-3}$ was observed in Guilford, United Kingdom, and the lowest median concentration of $94.3 \, \mu m^2 \, cm^{-3}$ was observed in Lund, Sweden. Comparing to the results of Pacitto et al. (2018), it has to be noted that in the study in question LDSA is defined as a surface area deposited in both the alveolar and the tracheobronchial region of the lungs, which leads to from 15 to 20 % increase in LDSA concentrations. The measured mean particle sizes are in line with previous research also reporting a majority of UFPs (Hussein et al., 2006; Buonanno et al., 2009).

350

355

However, in Cases from II to IV, the highest concentrations in the living room were observed after the cooking event. This phenomenon The peak number concentrations measured with DiSCmini were $1.05 \cdot 10^6$, $3.06 \cdot 10^4$, $6.12 \cdot 10^4$ and $4.09 \cdot 10^4$ cm⁻³ in Cases I to IV, respectively. These values can be compared to ones determined by Yeung and To (2008) for pan-frying chicken fillets in rapeseed oil using electric griddle. The comparison to the values of that study, ranging from $5.14 \cdot 10^5$ to $8.58 \cdot 10^5$ cm⁻³, confirms that, apart from Case I, the cooking emission was relatively low in this study. Additionally, the phenomenon that the peak concentration is reached after the cooking event indicates that the mixing and dispersion process of cooking-generated particles into the living room requires time. In addition, freshly cooked food is likely to produce particles that might increase LDSA concentration notably when food is not under an actively operated range hood.

After the peak concentration, LDSA concentration starts to decay slowly requiring several hours in all Cases. Simultaneously, the geometric mean of particle diameter increases, for instance, as the deposition coefficient of UFPs is higher than that of accumulation mode particles (Lai, 2002). In addition, coagulation increases the particle size especially in high particle concentrations as in Case I, where the role of coagulation can be observed as a higher increase rate of particle size compared to other Cases. During the decay process, LDSA concentration of different rooms of the dwellings, measured using the backpack, varied greatly. Mainly, the concentrations remained highest in the kitchen and the living room, but in Case I the concentration in the bathroom was observed to be the highest after approximately 2 hours of decay. Throughout the measurements, outdoor LDSA concentrations were stable compared to indoor concentrations in all Cases. Both the highest mean concentration and the highest standard deviation were measured in Case I, as expected. Overall, the outdoor concentrations were low in comparison to globally typical outdoor LDSA concentrations (Pacitto et al., 2021; Lepistö et al., 2023).

4.2 Utilization of the decay functions

360

365

380

385

390

The evaluation of the decay functions derived in Sect. 2 is conducted by fitting the functions to LDSA concentrations of the living room in Cases from I to IV. The living room data are chosen because it has better continuity compared to the backpack data that includes including measurements in different rooms. As noted in Sect. 4.1, in Cases from II to IV, the LDSA concentration of the living room increases after the cooking event has ended. Additionally, especially in Case IV, there is a strong variation in LDSA concentration after the peak value suggesting that the aerosol is not well mixed. Because the functions are not able to describe both the increase of concentration resulted from a periodic source and the decay of concentration within one fit, and the functions include assumption that the aerosol is well mixed, these observations indicate These observations confirm that the fitting of the decay functions cannot always start immediately after the cooking event.

To solve this challenge, a mixing phase is introduced as a time period that includes both the potential concentration increase and the mixing related variation of concentration. The length of the mixing phase is determined by an algorithm based on the normalized root mean square error (NRMSE) of a fitted decay function following Eq. (21). The normalization is performed using the mean value of data points, and the decay function including coagulation is selected for the algorithm because the highest concentrations, where coagulation might have a substantial role, are typically measured in the mixing phase. In the algorithm, the decay function is fitted to the time series of LDSA concentration using a non-linear least squares method and with a varying starting point. In the first fit, the starting point is the first measurement point after the cooking event and then it is shifted 5 seconds forward in every fit covering the first 20 minutes following the cooking event. The _as suggested in Sect. 3.2. To find suitable starting points to the fitting of the decay functions, algorithm introduced in Sect. 3.2 was utilized. In each Case, the relative deviation from minimum NRMSE in each Case, which determines the length of the mixing phase, is presented in Fig. 3, which shows that the NRMSEs stabilize near the minimum at a certain Case dependent time indicating the length of the mixing phase. In the algorithm, the starting point of the first fit having NRMSE within 10 % of the minimum NRMSE in each Case is defined as the end point of the mixing phase. The lengths of the mixing phases determined by the algorithm ranged from 35 seconds in Case I to 14 minutes and 58 seconds in Case IV. The mixing phases are presented with gray highlighting in Fig. 4.

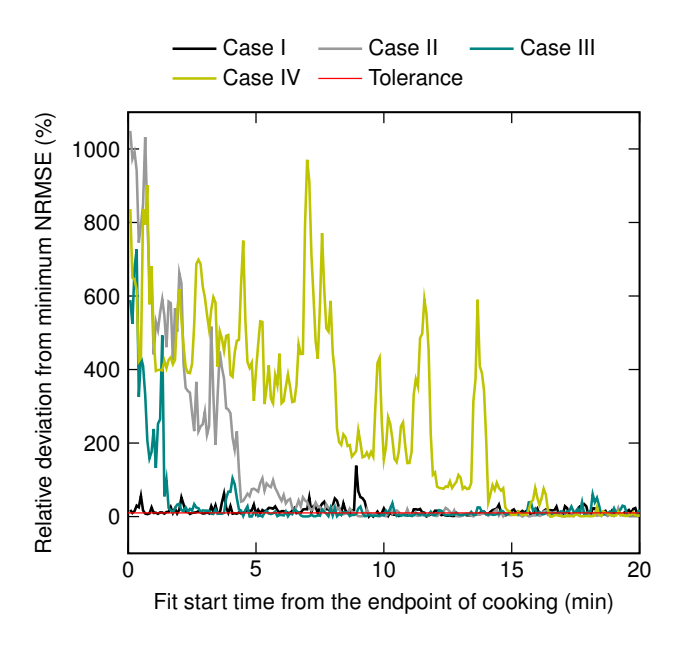


Figure 3. The relative deviation of NRMSEs of the decay function, following Eq. (21), from minimum NRMSE in Cases from I to IV. The first NRMSE of each Case that equals or is below the tolerance of 10 % determines the end point of the mixing phase.

After the determination of the mixing phase, the decay functions can be utilized using the data points of the decay phase following the mixing phase. Before fitting the functions, the background LDSA concentration $C_{\rm LDSA,i,bg}$ and the initial LDSA concentration of the decay phase $C_{\rm LDSA,i,0}$ have to be determined. The background concentrations were computed as the mean concentration of the background measurement in each living room, whereas the initial concentrations were defined as the concentration of the first data point in each decay phase. Using these values that are equal for both decay functions in each Case, the decay functions following Eq. (8) and Eq. (21) were fitted to the data of the decay phases. The fits of the decay function following Eq. (21) and, thus, considering coagulation are presented in Fig. 4 together with the initial concentrations, the background concentrations, and the fitting parameters $D_{\rm LDSA}$ and $K_{\rm LDSA}$ that stand for the dilution coefficient and the coagulation coefficient of LDSA concentration, respectively. Corresponding figure for the decay functions following Eq. (8) is presented in Supplement S3. In the fitting, the coefficients has have to be assumed constant throughout the decay process, although in reality they would vary due to the slow increase of GMD over time. In addition, the fitting errors of both decay functions are given in Table 3.

395

400

405

Looking at Fig. 4 and Table 3, both decay functions are found to fit the measurement data with a high accuracy. In Case I, the mean absolute errors (MAE) of both fits are notably higher compared to other Cases, but the values of NRMSE and R² indicate that the difference in magnitudes is explained by the overall higher level of concentration in Case I. Thus, the applicability of the theoretically derived decay functions is confirmed in a real-world environment. However, the decay functions following Eq. (21), that consider coagulation in addition to ventilation and deposition, produce systematically an equal or lower fitting error than the fits based on Eq. (8), only considering ventilation and deposition. Moreover, the relative difference between the

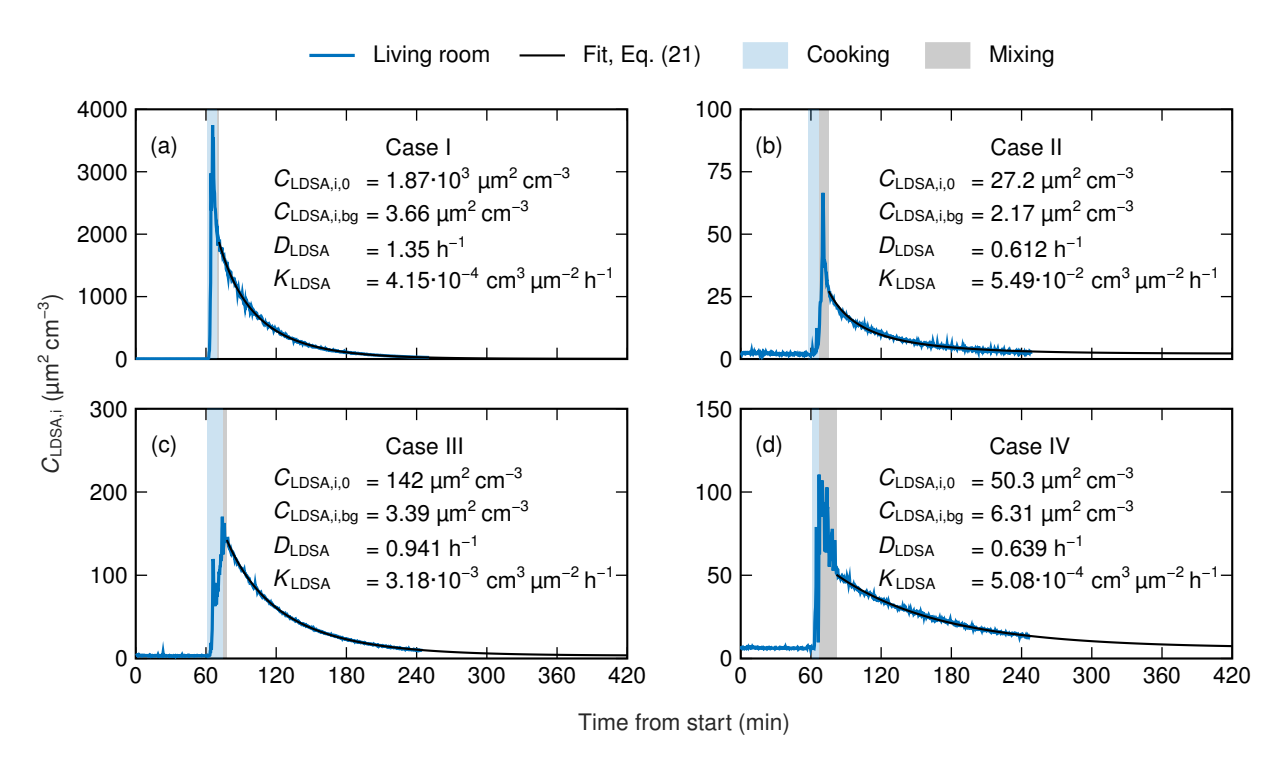


Figure 4. The fits and the fitting parameters of the decay function considering coagulation and following Eq. (21) in Cases I (a), II (b), III (c), and IV (d). Cooking events and mixing phases are highlighted.

Table 3. Mean absolute errors (MAE), normalized root mean square errors (NRMSE) and the coefficient of determination (\mathbb{R}^2) of the fits of the decay functions in Cases from I to IV. The decay function following Eq. (8) does not consider coagulation, whereas the function based on Eq. (21) includes coagulation.

Coagulation not considered, Eq. (8)			Coagulation considered, Eq. (21)			
MAE $(\mu \text{m}^2 \text{ cm}^{-3})$	NRMSE	\mathbb{R}^2	MAE $(\mu \text{m}^2 \text{ cm}^{-3})$	NRMSE	\mathbb{R}^2	
27.2	0.0951	0.994	10.8	0.0545	0.998	
0.800	0.134	0.964	0.465	0.0792	0.988	
1.92	0.0510	0.996	0.628	0.0215	0.999	
0.578	0.0296	0.994	0.575	0.0296	0.994	
	MAE (μm² cm ⁻³) 27.2 0.800 1.92	MAE $(μm^2 cm^{-3})$ NRMSE 27.2 0.0951 0.800 0.134 1.92 0.0510	$\begin{array}{c cccc} MAE & NRMSE & R^2 \\ \hline 27.2 & 0.0951 & 0.994 \\ 0.800 & 0.134 & 0.964 \\ 1.92 & 0.0510 & 0.996 \\ \hline \end{array}$	MAE (μm² cm⁻³) NRMSE $R²$ MAE (μm² cm⁻³) 27.2 0.0951 0.994 10.8 0.800 0.134 0.964 0.465 1.92 0.0510 0.996 0.628	MAE (μm² cm⁻³) NRMSE R² MAE (μm² cm⁻³) NRMSE 27.2 0.0951 0.994 10.8 0.0545 0.800 0.134 0.964 0.465 0.0792 1.92 0.0510 0.996 0.628 0.0215	

410 MAEs of the different decay functions is highest in Cases I and III with the highest initial concentrations. This observation is consistent with the fact that coagulation has a non-negligible role only in high number concentrations. According to the

DiSCmini, in Cases II and IV, the initial number concentrations $1.04 \cdot 10^4 \text{ cm}^{-3}$ and $1.19 \cdot 10^4 \text{ cm}^{-3}$, respectively, are at the limit where coagulation starts to act as a notable aerosol process.

The values of coagulation coefficient $K_{\rm LDSA}$, presented in Fig. 4, vary widely between Cases. It has to be noted that the intensity of coagulation with the monodisperse approximation the effect of coagulation on LDSA concentration depends more strongly, quadratically, on particle concentration as stated in Eq. (16). For instance, in Case I, the intensity effect of coagulation is approximately 40 times higher greater at the beginning of the decay phase compared to Case II despite of the two orders of magnitude lower value of the coagulation coefficient. Using Eq. (17), the coagulation coefficients of this study can be compared to ones determined to number concentration in earlier studies. For instance, the mean coagulation coefficient of $7.8 \cdot 10^{-6} \, h^{-1}$, determined by Zhao et al. (2021), corresponds to LDSA coagulation coefficient of $6.39 \cdot 10^{-4} \, {\rm cm}^3 \, {\rm \mu m}^{-2} \, h^{-1}$, which is of the same order of magnitude as the coefficients of Cases I and IV. Consequently, it remains unclear whether the fit function following Eq. (21) is able to determine the coagulation coefficient accurately especially in low particle concentrations in which the role of coagulation as an aerosol process is minor.

In contrast to the coagulation coefficients, the dilution coefficients are of the same order of magnitude in all Cases. At the same time, even minor differences in dilution coefficients have a significant effect on the dilution rate, especially in lower concentrations. This is demonstrated by the fact that, in Case IV, LDSA concentration at 420 minutes predicted by the fit of Eq. (21) is highest above the background concentration even though the initial concentration is relatively low. Although Case II has the lowest dilution coefficient, the high coagulation coefficient and the initially low concentration result in faster decay near to the background level compared to Case IV.

Overall, despite the differences in dilution and coagulation coefficients, the duration of the decay process is long in all Cases from I to IV taking 231, 223, 182, and 283 minutes, respectively, for the concentration of living room, predicted by the fit of Eq. (21), to decrease below the mean outdoor concentration of each Case presented in Fig. 2. This observation already emphasizes the need for a decay function to asses the total exposure to cooking-generated particles instead of the exposure only during the active cooking event.

435 **4.3** Outdoor air quality

425

440

The outdoor air quality data of Tampere was utilized in the dose calculation described in Sect. 3.3. The outdoor LDSA concentrations measured at the two measurement stations of Tampere city, Epilä and Pirkankatu, are relatively low with the annual mean values of 8.4 and 9.2 μm^2 cm⁻³, respectively. Globally, the outdoor LDSA concentrations of urban background and traffic environments are at the level of 30 μm^2 cm⁻³ or higher(Kuula et al., 2020; Lepistö et al., 2023). Even values above, reaching up to over 300 μm^2 cm⁻³ have been reported in Santiago, Chile, (Lepistö et al., 2023) and Delhi National Capital Region, India (Salo et al., 2021)(Kuula et al., 2020; Salo et al., 2021; Lepistö et al., 2023). However, in Finland and Switzerland, urban background concentrations around 10 μm^2 cm⁻³ have been reported in earlier studies (Kuula et al., 2020; Kuuluvainen et al., 2016; Fierz et al., 2011).

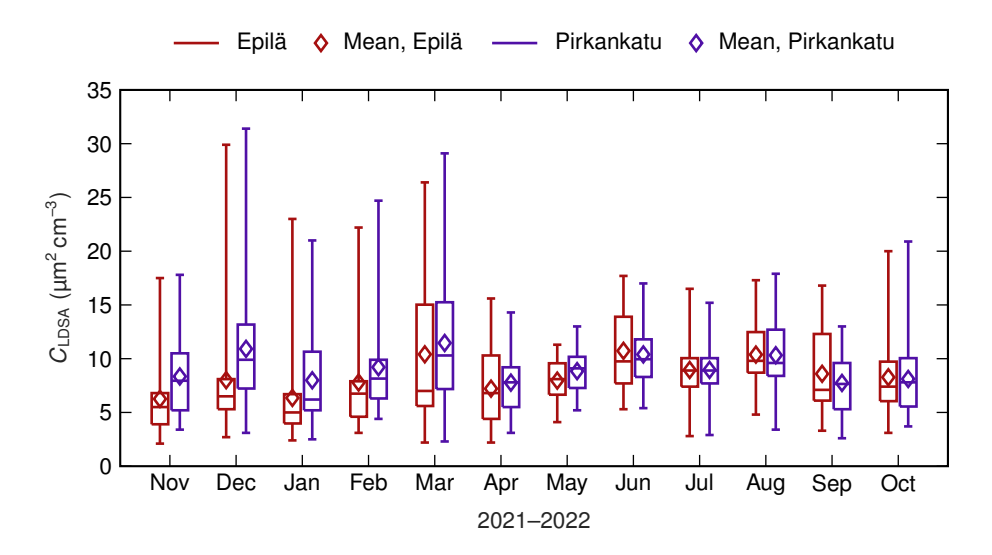


Figure 5. The monthly variation of the daily averages of LDSA concentration in two outdoor air quality measurement stations, Epilä and Pirkankatu, located in Tampere. 25th and 75th percentiles, median values, mean values, and the ranges of variation are presented as boxes, horizontal lines, diamonds, and whiskers, respectively.

The monthly variation of the daily averages of LDSA concentration in two outdoor air quality measurement stations, Epilä and Pirkankatu, located in Tampere. 25th and 75th percentiles, median values, mean values, and the ranges of variation are presented as boxes, horizontal lines, diamonds, and whiskers, respectively.

The seasonal variation of LDSA concentrations of both stations, illustrated in Fig. 5, is moderate as the median and the mean values of daily averages range from 5.0 to 11.5 μm^2 cm⁻³. Nonetheless, concentrations are slightly elevated during the summer months, June, July, and August, corresponding to the seasonal variation in Helsinki, Finland, reported by Kuula et al. (2020). Elevated concentrations are also observed in March for both stations and in December at Pirkankatu. Additionally, the highest individual daily concentrations were measured in winter and early spring, from December to March. During the snow coverage starting in November and ending at the turn of March and April, the concentrations at Pirkankatu are also notably higher than those at Epilä in contrast to the months of unfrozen ground.

450

460

The diurnal cycle of LDSA concentrations of both measurement stations shows similarity to earlier studies (Hama et al., 2017; Kuula et al., 2020). During weekdays, the daily time series is bi-modal having the first peak in the morning and the second peak in the afternoon, whereas during weekends only the afternoon peak is observed. In both studies, these peaks have been connected to the intensity of traffic. Consequently, it is unsurprising that LDSA concentrations are lower during the nighttime with the mean of 7.3 µm² cm⁻³, while the mean daytime concentration was 9.5 µm² cm⁻³. In this study the daytime is was defined as a time period between 7:00 and 23:00, and the mean values of day and night are calculated using a year's worth of data from both measurement stations. During daytime, the seasonal variation in the diurnal cycle is minor, but at night LDSA concentration significantly decreases during winter, whereas in summer, the concentration remains close to the

daytime levels. The above described mean daytime and nighttime LDSA concentrations of Tampere were utilized in the dose calculation.

4.4 Dose assessment

The daily LDSA dose received by the population of Tampere region can be was assessed by combining the results of cooking measurements, the fits of the decay functions and the observations of outdoor air quality according to the describtion of Sect. 3.3. As a result, the assessment provides knowledge of the role that cooking and especially the decay phase of the cooking-generated particles have in the total daily exposuredaily particle dose. In earlier LDSA studies, only the exposure during cooking or eating is considered as cooking related exposure (Buonanno et al., 2011; Pacitto et al., 2018; Scungio et al., 2020; Pacitto et al., 2021), although the decay phase of cooking-generated particles may last from an hour to several hours as demonstrated in this study and previous research (Hussein et al., 2006; Wan et al., 2011) (Hussein et al., 2006; Wan et al., 2011; Zhao et al., 2021)

The total exposure to cooking-generated particles is calculated by summing LDSA doses during the cooking, mixing, and extrapolated decay phases. The decay phase is extrapolated using the fitted decay function and the LDSA doses $\delta_{\rm LDSA}$ are determined using equation-

$$\delta_{\rm LDSA} = {\rm IR} \int_{t_0}^{t_1} C_{\rm LDSA} \; \mathrm{d}t,$$

475

480

where IR is the inhalation rate (IR), while t_0 and t_1 are the start and the end point of the phase, respectively. The daytime IR of 16.3 is computed as the average IR excluding sleep or nap time for individuals aged from 21 to 60 years based on the statistics of EPA (2009). In the case of cooking and mixing phase, the integrand is the LDSA concentration of the living room subtracted by the mean indoor background concentration. The integration is performed numerically using the trapezoidal rule. The dose of the extrapolated decay phase is computed using the integral of the background term subtracted fits of Eq. (8) and Eq. (21). To get the total dose of the extrapolated decay phase, the integral of Eq. (22) is calculated from the starting point of the decay phase to infinity. Despite integrating to infinity, the total dose of one cooking event is suitable for assessing daily exposure because in all Cases the integral increases under 1 % after 12 hours of decay.

The outdoor air quality data of Tampere are utilized to estimate the average background doses of indoor and outdoor environments. As the mean LDSA concentrations of day and night, presented in Sect. 4.3, are used to compute the background doses, Eq. (22) can be simplified to form

$$\delta_{\text{LDSA}} = \text{IR}\overline{C}_{\text{LDSA}}\Delta t,$$

where $\overline{C}_{\text{LDSA}}$ is the average LDSA concentration and Δt is the time spent in a certain environment. The estimate for the indoor dose is computed in two parts using Eq. (23). First, the indoor dose during the night is calculated using the nighttime mean concentration of Tampere's air quality stations and I/O-ratio of 0.44, which has been determined by Silvonen et al. (2023) for an office building located in Tampere.

In the calculation of the nightly indoor dose, the length of a night was assumed to be 8 hours and the average sleep or nap IR of 4.8 (EPA, 2009) was used. Secondly, the indoor dose during daytime is computed from the daytime mean concentration of Tampere using the I/O-ratio, the daytime IR, and the average time spent indoors in Finland provided by Hussein et al. (2012). The sleep time of 8 hours is subtracted from the indoor-spent time of 21 hours and 26 minutes.

495

500

505

515

520

525

The results of the dose ealculations described above assessment are presented in Fig. 6 for both decay functions. Using the decay function following Eq. (8), the total daily doses are 1389, 104.5, 215.3, and 162.5 mm² in Cases from I to IV, respectively. However, in all Cases, the utilization of the decay function following Eq. (21) gives slightly higher doses with corresponding values of 1422, 105.9, 218.7, and 162.8 mm², respectively. Apart form Case IV, the fits of Eq. (8) are observed to give values lower than the measured ones at the end of the measurement, whereas the values of the fits of Eq. (21) are in better agreement with the measurements. This observation explains the differences between the decay functions in both the daily doses of Fig. 6 and fitting errors of Table 3. Together with the fitting errors, it indicates that the decay function taking coagulation into account is likely to give a better estimate of the actual dose of cooking-generated particles. It has to be noted that the relative differences in the doses are minor, which makes also the simpler decay function applicable for assessing the total dose of a cooking event.

Compared to previous studies with a higher number of measurement cases (Pacitto et al., 2018; Scungio et al., 2020; Pacitto et al., 2021), the daily doses in Cases from II to IV are closest to ones measured in Lund, Sweden, where the daily doses for female and male were on average 102 and 93 mm², respectively. Despite differing substantially from other daily doses of this study, the daily dose of Case I has similarity with doses determined in Guilford, United Kingdom, and Cairo, Egypt. In Guilford, the daily doses of female and male are 1408 and 1188 mm², respectively, and in Cairo, the corresponding doses are 1306 and 1309 mm², respectively. It has to be noted that in those studies, unlike in this study, the particle surface area deposited at the tracheobronchial region of the lungs is also included in LDSA leading to from 15 to 20 % higher values of LDSA (Pacitto et al., 2018).

With both decay functions, the cooking-related particle exposure—dose fraction, presented in Fig. 6, varies greatly between Cases. The highest In this study, the cooking-related particle dose considers cooking and mixing phase together with extrapolated decay phase. The highest cooking-related fraction of 93.9 % is observed in Case I using the decay function following Eq. (21), while the lowest fraction of 17.2 % is determined in Case II using the decay function based on Eq. (8). This variation observed with identical ingredients indicates that the ventilation and the style of cooking may have a significant impact on the total exposure—dose of the cooking event. Overall, the dose exposure assessment shows that, in the Tampere region, a notable fraction of daily exposure—the daily dose relates to cooking that even has a dominant role in two of the four Cases. In all Cases, most of the dose is received in the decay phase, not during the actual cooking event. The fraction of the extrapolated decay phase dose from the total cooking dose varies from 66.5 % to 80.3 % using the decay function that follows Eq. (8) and from 72.9 % to 82.9 % using the decay function following Eq. (21). Consequently, it is clear that considering only the active cooking event is not enough to determine the total exposure—particle dose of cooking.

Because of this, the role of cooking might have been underestimated in earlier studies even though it has been recognized as a major source of particle exposure (Pacitto et al., 2018; Scungio et al., 2020; Pacitto et al., 2021). Pacitto et al. (2021) reported

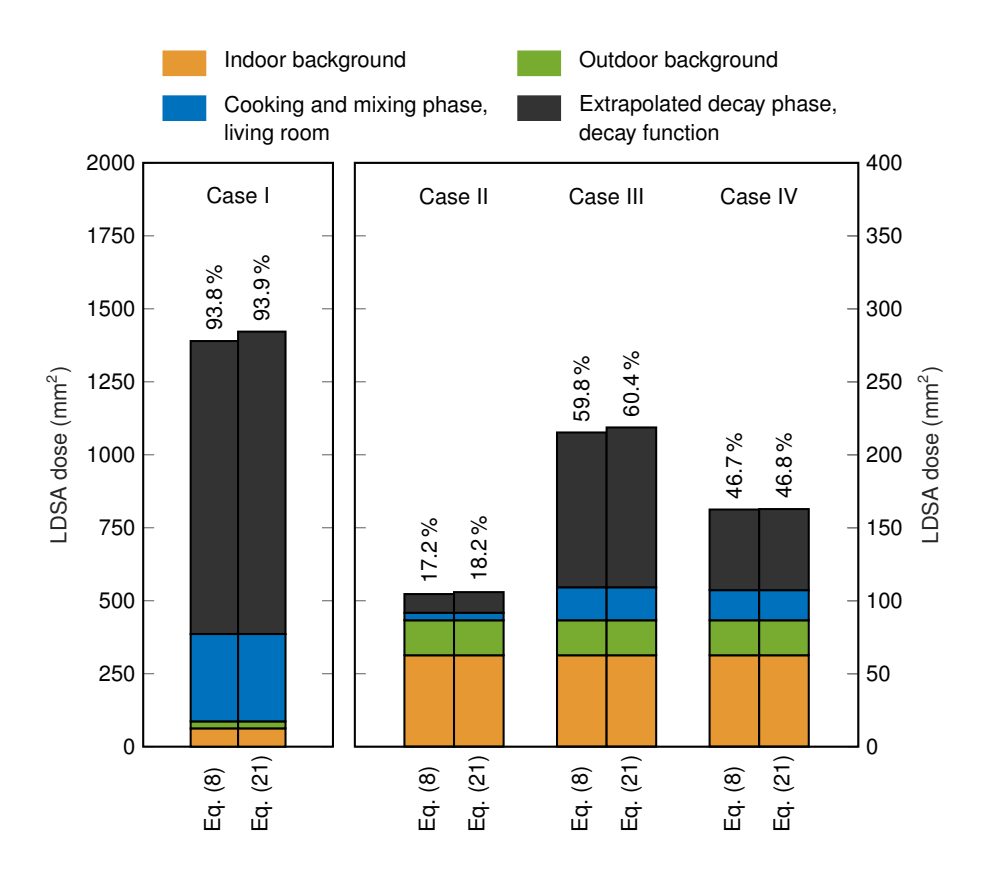


Figure 6. Daily LDSA doses in Cases from I to IV consisting of indoor background, outdoor background, cooking and mixing phase in the living room, and extrapolated decay phase separately with decay functions following Eq. (8) and (21). The fraction of cooking related dose, including cooking, mixing and extrapolated decay phase, is presented numerically. Note that Case I has a separate y-axis due to higher values.

that in developed countries the average contribution of cooking and eating actions varies between 14 %, for males in Barcelona, Spain, and 59 %, for females in Cassino, Italy. However, the dose fraction is highly dependent on the dose received from other sources such as traffic and outdoor air. For instance, the average daily dose from cooking and eating for females in Cassino was assessed to be 779 mm² (Pacitto et al., 2018, 2021), while in Case III, similar dose fractions are achieved with cooking related doses of approximately 130 mm². Apart from Case I, the LDSA doses related to cooking show similarity to cooking and eating doses measured in Barcelona, ranging from 61 to 178 mm², and Lund, ranging from 30 to 67 mm² (Pacitto et al., 2018). However, it is challenging to assess which fraction of the dose received during the decay phase of cooking-generated particles is taken into account during eating periods. Consequently, the consideration of the whole decay phase might further increase the already significant role of cooking-related particles in the total daily dose.

530

5 Summary and conclusions

540

545

550

555

In this study, two decay functions describing indoor LDSA concentration were first derived and then tested using measurement data of four cooking experiments including the decay phase of the cooking emission. Both functions were confirmed to fit the measured data with a high accuracy, but using the decay function that considers coagulation, in addition to ventilation and deposition, the fitting errors were systematically lower. The difference in the errors was emphasized in the cases of high concentration.

Together with air quality data of Tampere, the fits of the decay functions were applied to assess the role of cooking in the daily LDSA exposuredose. The fraction of cooking related LDSA dose varied from 17.2 to 93.9 % highlighting both the significance of cooking exposure on total exposure the cooking dose on total particle dose and the great influence that cooking style and ventilation may have on the received dose. However, the primary finding was that, using the simpler decay function, from 66.5 to 80.3 % and, using the decay function considering coagulation, from 72.9 to 82.9 % of the cooking-related dose was received at the decay phase following the active cooking event and the mixing phase. Consequently, it is crucial to consider the particles of the decay phase as cooking-related emissions when assessing the role of cooking in the daily particle exposure.

Using the decay functions of this study, also the measurement data of a low time resolution or a short time period can be interpolated or extrapolated providing a useful tool for assessing the exposure at the decay phase. The decay functions could also be utilized to describe the decay processes of other indoor particle sources noting that, in the more complex decay function, the consideration of coagulation includes the assumption that the size distribution is dominated by particles with diameter in the range of 30 to 300 nm. Consequently, as most of the indoor sources produce particles within that size range, the decay functions can be applied to distinguish the emissions of successive indoor emission events from each other. Furthermore, the factors affecting the decay process of indoor emissions, such as ventilation systems and the usage of range hoods, can be examined more in detail using the decay functions. To achieve these potential improvements in the knowledge, more extensive studies of indoor LDSA concentrations including the decay phase of indoor particle emissions are required.

Data availability. Data are available from Zenodo at: https://doi.org/10.5281/zenodo.15471503 (Vesisenaho et al., 2025)

Author contributions. KV: conceptualization, investigation, data curation, methodology, formal analysis, software, visualization, writing (original draft preparation), writing (review and editing) HK and PK: conceptualization, investigation, supervision, writing (review and editing) UVM: conceptualization, investigation, data curation, writing (review and editing) MO: conceptualization, investigation, writing (review and editing)

Competing interests. The authors declare that they have no conflict of interest.

Acknowledgements. The authors would like to thank the City of Tampere's Environmental Protection Unit for measuring LDSA concentrations as a part of Tampere's urban air quality monitoring. In addition, authors would like to thank Pegasor Ltd for maintaining the AQ Urban sensors annually.

References

- Abdullahi, K. L., Delgado-Saborit, J. M., and Harrison, R. M.: Emissions and indoor concentrations of particulate matter and its specific chemical components from cooking: A review, Atmospheric Environment, 71, 260 294, https://doi.org/10.1016/j.atmosenv.2013.01.061, 2013.
 - Ahmed, T., Kumar, P., and Mottet, L.: Natural ventilation in warm climates: The challenges of thermal comfort, heatwave resilience and indoor air quality, Renewable and sustainable energy reviews, 138, 110 669, https://doi.org/10.1016/j.rser.2020.110669, 2021.
- Bhangar, S., Mullen, N., Hering, S., Kreisberg, N., and Nazaroff, W. W.: Ultrafine particle concentrations and exposures in seven residences in northern California, Indoor Air, 21, 132 144, https://doi.org/10.1111/j.1600-0668.2010.00689.x, 2011.
 - Buonanno, G., Morawska, L., and Stabile, L.: Particle emission factors during cooking activities, Atmospheric Environment, 43, 3235 3242, https://doi.org/10.1016/j.atmosenv.2009.03.044, 2009.
 - Buonanno, G., Giovinco, G., Morawska, L., and Stabile, L.: Tracheobronchial and alveolar dose of submicrometer particles for different population age groups in Italy, Atmospheric Environment, 45, 6216 6224, https://doi.org/10.1016/j.atmosenv.2011.07.066, 2011.
- Burnett, R., Chen, H., Szyszkowicz, M., Fann, N., Hubbell, B., Pope Iii, C. A., Apte, J. S., Brauer, M., Cohen, A., Weichenthal, S., Coggins, J., Di, Q., Brunekreef, B., Frostad, J., Lim, S. S., Kan, H., Walker, K. D., Thurston, G. D., Hayes, R. B., Lim, C. C., Turner, M. C., Jerrett, M., Krewski, D., Gapstur, S. M., Diver, W. R., Ostro, B., Goldberg, D., Crouse, D. L., Martin, R. V., Peters, P., Pinault, L., Tjepkema, M., Van Donkelaar, A., Villeneuve, P. J., Miller, A. B., Yin, P., Zhou, M., Wang, L., Janssen, N. A., Marra, M., Atkinson, R. W., Tsang, H., Thach, T. Q., Cannon, J. B., Allen, R. T., Hart, J. E., Laden, F., Cesaroni, G., Forastiere, F., Weinmayr, G., Jaensch, A., Nagel, G., Concin,
- 585 H., and Spadaro, J. V.: Global estimates of mortality associated with longterm exposure to outdoor fine particulate matter, Proceedings of the National Academy of Sciences of the United States of America, 115, 9592 9597, https://doi.org/10.1073/pnas.1803222115, 2018.
 - Chen, J. and Hoek, G.: Long-term exposure to PM and all-cause and cause-specific mortality: A systematic review and meta-analysis, Environment International, 143, https://doi.org/10.1016/j.envint.2020.105974, 2020.
- Cohen, A., Brauer, M., Burnett, R., Anderson, H. R., Frostad, J., Estep, K., Balakrishnan, K., Brunekreef, B., Dandona, L., Dandona, R.,
 Feigin, V., Freedman, G., Hubbell, B., Jobling, A., Kan, H., Knibbs, L., Liu, Y., Martin, R., Morawska, L., Pope, C. A., Shin, H., Straif, K., Shaddick, G., Thomas, M., van Dingenen, R., van Donkelaar, A., Vos, T., Murray, C. J. L., and Forouzanfar, M. H.: Estimates and 25-year trends of the global burden of disease attributable to ambient air pollution: an analysis of data from the Global Burden of Diseases Study 2015, The Lancet (British edition), 389, 1907–1918, https://doi.org/10.1016/S0140-6736(17)30505-6, 2017.
- Crump, J. G., Flagan, R. C., and Seinfeld, J. H.: Particle wall loss rates in vessels, Aerosol Science and Technology, 2, 303 309, https://doi.org/10.1080/02786828308958636, 1982.
 - Dimitroulopoulou, C.: Ventilation in European dwellings: A review, Building and Environment, 47, 109 125, https://doi.org/10.1016/j.buildenv.2011.07.016, 2012.
 - Donaldson, K., Brown, D., Clouter, A., Duffin, R., MacNee, W., Renwick, L., Tran, L., and Stone, V.: The pulmonary toxicology of ultrafine particles, Journal of Aerosol Medicine: Deposition, Clearance, and Effects in the Lung, 15, 213 220, https://doi.org/10.1089/089426802320282338, 2002.
 - EPA: Metabolically derived human ventilation rates: a revised approach based upon oxygen consumption rates, Tech. Rep. EPA/600/R-06/129F, U.S. Environmental Protection Agency, National Center for Environmental Assessment, 2009.
 - EPA: National Ambient Air Quality Standards for Particulate Matter, Federal Register, 78, https://www.govinfo.gov/content/pkg/FR-2013-01-15/pdf/2012-30946.pdf, last access: 13 June 2024, 2013.

- 605 EPA: Exposure Factors Handbook 2011 Edition (Final Report), U.S. Environmental Protection Agency, 2011.
 - EU: Directive 2008/50/EC of the European Parliament and of the Council of 21 May 2008 on ambient air quality and cleaner air for Europe, Official Journal of the European Union, http://data.europa.eu/eli/dir/2008/50/oi, last access: 13 June 2024, 2008.
 - Eurostat: Population on 1 January by age groups and sex cities and greater cities, Eurostat [data set], https://doi.org/10.2908/URB_CPOP1, 2024.
- 610 Fierz, M., Houle, C., Steigmeier, P., and Burtscher, H.: Design, calibration, and field performance of a miniature diffusion size classifier, Aerosol Science and Technology, 45, 1 10, https://doi.org/10.1080/02786826.2010.516283, 2011.
 - Fierz, M., Meier, D., Steigmeier, P., and Burtscher, H.: Aerosol measurement by induced currents, Aerosol Science and Technology, 48, 350 357, https://doi.org/10.1080/02786826.2013.875981, 2014.
- Geiss, O., Bianchi, I., and Barrero-Moreno, J.: Lung-deposited surface area concentration measurements in selected occupational and non-occupational environments, Journal of Aerosol Science, 96, 24 37, https://doi.org/10.1016/j.jaerosci.2016.02.007, 2016.
 - Hama, S. M., Ma, N., Cordell, R. L., Kos, G. P., Wiedensohler, A., and Monks, P. S.: Lung deposited surface area in Leicester urban background site/UK: Sources and contribution of new particle formation, Atmospheric Environment, 151, 94 107, https://doi.org/10.1016/j.atmosenv.2016.12.002, 2017.
- Hussein, T., Glytsos, T., Ondráček, J., Dohányosová, P., Ždímal, V., Hämeri, K., Lazaridis, M., Smolík, J., and Kulmala, M.: Par-620 ticle size characterization and emission rates during indoor activities in a house, Atmospheric Environment, 40, 4285 – 4307, https://doi.org/10.1016/j.atmosenv.2006.03.053, 2006.
 - Hussein, T., Hruška, A., Dohányosová, P., Džumbová, L., Hemerka, J., Kulmala, M., and Smolík, J.: Deposition rates on smooth surfaces and coagulation of aerosol particles inside a test chamber, Atmospheric Environment, 43, 905 914, https://doi.org/10.1016/j.atmosenv.2008.10.059, 2009.
- Hussein, T., Paasonen, P., and Kulmala, M.: Activity pattern of a selected group of school occupants and their family members in Helsinki Finland, The Science of the total environment, 425, 289 292, https://doi.org/10.1016/j.scitotenv.2012.03.002, 2012.
 - Hänninen, O. O., Palonen, J., Tuomisto, J. T., Yli-Tuomi, T., Seppänen, O., and Jantunen, M. J.: Reduction potential of urban PM2.5 mortality risk using modern ventilation systems in buildings, Indoor Air, 15, 246 256, https://doi.org/10.1111/j.1600-0668.2005.00365.x, 2005.
 - ICRP: Human respiratory tract model for radiological protection. A report of a Task Group of the International Commission on Radiological Protection., Annals of the ICRP, 24, 1 482, 1994.

- Isaxon, C., Gudmundsson, A., Nordin, E., Lönnblad, L., Dahl, A., Wieslander, G., Bohgard, M., and Wierzbicka, A.: Contribution of indoorgenerated particles to residential exposure, Atmospheric Environment, 106, 458 466, https://doi.org/10.1016/j.atmosenv.2014.07.053, 2015.
- Kang, K., Kim, H., Kim, D. D., Lee, Y. G., and Kim, T.: Characteristics of cooking-generated PM10 and PM2.5 in residential buildings with different cooking and ventilation types, Science of the Total Environment, 668, 56 66, https://doi.org/10.1016/j.scitotenv.2019.02.316, 2019.
 - Kanninen, K., Lampinen, R., Rantanen, L., Odendaal, L., Jalava, P., Chew, S., and White, A.: Olfactory cell cultures to investigate health effects of air pollution exposure: Implications for neurodegeneration, Neurochemistry International, 136, 104729, https://doi.org/10.1016/j.neuint.2020.104729, 2020.
- 640 Kim, H., Kang, K., and Kim, T.: Measurement of particulate matter (PM2.5) and health risk assessment of cooking-generated particles in the kitchen and living rooms of apartment houses, Sustainability (Switzerland), 10, https://doi.org/10.3390/su10030843, 2018.

- Kim, K.-H., Kabir, E., and Kabir, S.: A review on the human health impact of airborne particulate matter, Environment international, 74, 136–143, https://doi.org/10.1016/j.envint.2014.10.005, 2015.
- Kuula, J., Kuuluvainen, H., Rönkkö, T., Niemi, J. V., Saukko, E., Portin, H., Aurela, M., Saarikoski, S., Rostedt, A., Hillamo, R., and
 Timonen, H.: Applicability of optical and diffusion charging-based particulate matter sensors to urban air quality measurements, Aerosol and Air Quality Research, 19, 1024 1039, https://doi.org/10.4209/aaqr.2018.04.0143, 2019.
 - Kuula, J., Kuuluvainen, H., Niemi, J. V., Saukko, E., Portin, H., Kousa, A., Aurela, M., Rönkkö, T., and Timonen, H.: Long-term sensor measurements of lung deposited surface area of particulate matter emitted from local vehicular and residential wood combustion sources, Aerosol Science and Technology, 54, 190 202, https://doi.org/10.1080/02786826.2019.1668909, 2020.
- Kuuluvainen, H., Rönkkö, T., Järvinen, A., Saari, S., Karjalainen, P., Lähde, T., Pirjola, L., Niemi, J. V., Hillamo, R., and Keskinen, J.: Lung deposited surface area size distributions of particulate matter in different urban areas, Atmospheric Environment, 136, 105 113, https://doi.org/10.1016/j.atmosenv.2016.04.019, 2016.
 - Lai, A.: Particle deposition indoors: A review, Indoor Air, 12, 211 214, https://doi.org/10.1046/j.0905-6947.2002.1r159a.x, 2002.
- Lepistö, T., Lintusaari, H., Oudin, A., Barreira, L. M., Niemi, J. V., Karjalainen, P., Salo, L., Silvonen, V., Markkula, L., Hoivala, J., Marjanen, P., Martikainen, S., Aurela, M., Reyes, F. R., Oyola, P., Kuuluvainen, H., Manninen, H. E., Schins, R. P., Vojtisek-Lom, M., Ondracek, J., Topinka, J., Timonen, H., Jalava, P., Saarikoski, S., and Rönkkö, T.: Particle lung deposited surface area (LDSAal) size distributions in different urban environments and geographical regions: Towards understanding of the PM2.5 dose–response, Environment International, 180, https://doi.org/10.1016/j.envint.2023.108224. 2023.
- Li, X., Jin, L., and Kan, H.: Air pollution: a global problem needs local fixes, Nature, 570, 437 439, https://doi.org/10.1038/d41586-019-01960-7, 2019.
 - Liu, Q., Xu, C., Ji, G., Liu, H., Shao, W., Zhang, C., Gu, A., and Zhao, P.: Effect of exposure to ambient PM2.5 pollution on the risk of respiratory tract diseases: A meta-analysis of cohort studies, Journal of Biomedical Research, 31, 130 142, https://doi.org/10.7555/JBR.31.20160071, 2017.
- Monteiller, C., Tran, L., MacNee, W., Faux, S., Jones, A., Miller, B., and Donaldson, K.: The pro-inflammatory effects of low-toxicity low-solubility particles, nanoparticles and fine particles, on epithelial cells in vitro: The role of surface area, Occupational and Environmental Medicine, 64, 609 615, https://doi.org/10.1136/oem.2005.024802, 2007.
 - Morawska, L., Afshari, A., Bae, G., Buonanno, G., Chao, C., Hänninen, O., Hofmann, W., Isaxon, C., Jayaratne, E., Pasanen, P., Salthammer, T., Waring, M., and Wierzbicka, A.: Indoor aerosols: From personal exposure to risk assessment, Indoor Air, 23, 462 487, https://doi.org/10.1111/ina.12044, 2013.
- Mullen, N. A., Liu, C., Zhang, Y., Wang, S., and Nazaroff, W. W.: Ultrafine particle concentrations and exposures in four high-rise Beijing apartments, Atmospheric Environment, 45, 7574 7582, https://doi.org/10.1016/j.atmosenv.2010.07.060, 2011.
 - $Nazaroff, W.\ W.:\ Indoor\ particle\ dynamics,\ Indoor\ Air,\ Supplement,\ 14,\ 175-183,\ https://doi.org/10.1111/j.1600-0668.2004.00286.x,\ 2004.00286.x,\ 2004.00286.x,$
 - Nazaroff, W. W. and Cass, G. R.: Mathematical Modeling of Indoor Aerosol Dynamics, Environmental Science and Technology, 23, 157 166, https://doi.org/10.1021/es00179a003, 1989.
- Nemmar, A., Hoet, P., Vanquickenborne, B., Dinsdale, D., Thomeer, M., Hoylaerts, M., Vanbilloen, H., Mortelmans, L., and Nemery, B.: Passage of inhaled particles into the blood circulation in humans, Circulation, 105, 411 414, https://doi.org/10.1161/hc0402.104118, 2002.

- Niculita-Hirzel, H.: Latest trends in pollutant accumulations at threatening levels in energy-efficient residential buildings with and without mechanical ventilation: A Review, International Journal of Environmental Research and Public Health, 19, 3538, https://doi.org/10.3390/ijerph19063538, 2022.
 - Oberdörster, G., Sharp, Z., Atudorei, V., Elder, A., Gelein, R., Kreyling, W., and Cox, C.: Translocation of inhaled ultrafine particles to the brain, Inhalation Toxicology, 16, 437 445, https://doi.org/10.1080/08958370490439597, 2004.
 - Oberdörster, G., Oberdörster, E., and Oberdörster, J.: Nanotoxicology: An emerging discipline evolving from studies of ultrafine particles, Environmental Health Perspectives, 113, 823 839, https://doi.org/10.1289/ehp.7339, 2005.
- Ohlwein, S., Kappeler, R., Kutlar Joss, M., Künzli, N., and Hoffmann, B.: Health effects of ultrafine particles: a systematic literature review update of epidemiological evidence, International Journal of Public Health, 64, 547 559, https://doi.org/10.1007/s00038-019-01202-7, 2019.
 - Pacitto, A., Stabile, L., Moreno, T., Kumar, P., Wierzbicka, A., Morawska, L., and Buonanno, G.: The influence of lifestyle on airborne particle surface area doses received by different Western populations, Environmental Pollution, 232, 113 122, https://doi.org/10.1016/j.envpol.2017.09.023, 2018.

- Pacitto, A., Stabile, L., Morawska, L., Nyarku, M., Torkmahalleh, M. A., Akhmetvaliyeva, Z., Andrade, A., Dominski, F. H., Mantecca, P., Shetaya, W. H., Mazaheri, M., Jayaratne, R., Marchetti, S., Hassan, S. K., El-Mekawy, A., Mohamed, E. F., Canale, L., Frattolillo, A., and Buonanno, G.: Daily submicron particle doses received by populations living in different low- and middle-income countries, Environmental Pollution, 269, https://doi.org/10.1016/j.envpol.2020.116229, 2021.
- Park, J., Jee, N.-Y., and Jeong, J.-W.: Effects of types of ventilation system on indoor particle concentrations in residential buildings, Indoor Air, 24, 629 638, https://doi.org/10.1111/ina.12117, 2014.
 - Rostedt, A., Arffman, A., Janka, K., Yli-Ojanperä, J., and Keskinen, J.: Characterization and response model of the PPS-M aerosol sensor, Aerosol Science and Technology, 48, 1022 1030, https://doi.org/10.1080/02786826.2014.951023, 2014.
- Salo, L., Hyvärinen, A., Jalava, P., Teinilä, K., Hooda, R. K., Datta, A., Saarikoski, S., Lintusaari, H., Lepistö, T., Martikainen, S., Rostedt,
 A., Sharma, V. P., Rahman, M. H., Subudhi, S., Asmi, E., Niemi, J. V., Lihavainen, H., Lal, B., Keskinen, J., Kuuluvainen, H., Timonen,
 H., and Rönkkö, T.: The characteristics and size of lung-depositing particles vary significantly between high and low pollution traffic
 environments, Atmospheric Environment, 255, https://doi.org/10.1016/j.atmosenv.2021.118421, 2021.
 - Schmid, O. and Stoeger, T.: Surface area is the biologically most effective dose metric for acute nanoparticle toxicity in the lung, Journal of Aerosol Science, 99, 133 143, https://doi.org/10.1016/j.jaerosci.2015.12.006, 2016.
- 705 Schraufnagel, D. E.: The health effects of ultrafine particles, Experimental and Molecular Medicine, 52, 311 317, https://doi.org/10.1038/s12276-020-0403-3, 2020.
 - Scungio, M., Rizza, V., Stabile, L., Morawska, L., and Buonanno, G.: Influence of methodology on the estimation of the particle surface area dose received by a population in all-day activities, Environmental Pollution, 266, https://doi.org/10.1016/j.envpol.2020.115209, 2020.
- Silvonen, V., Salo, L., Raunima, T., Vojtisek-Lom, M., Ondracek, J., Topinka, J., Schins, R. P., Lepistö, T., Lintusaari, H., Saarikoski, S., Barreira, L. M., Hoivala, J., Markkula, L., Kulmala, I., Vinha, J., Karjalainen, P., and Rönkkö, T.: Lung-depositing surface area (LDSA) of particles in office spaces around Europe: Size distributions, I/O-ratios and infiltration, Building and Environment, 246, https://doi.org/10.1016/j.buildenv.2023.110999, 2023.
- Tang, R., Sahu, R., Su, Y., Milsom, A., Mishra, A., Berkemeier, T., and Pfrang, C.: Impact of Cooking Methods on Indoor Air Quality: A Comparative Study of Particulate Matter (PM) and Volatile Organic Compound (VOC) Emissions, Indoor Air, 2024, https://doi.org/10.1155/2024/6355613, 2024.

- Todea, A. M., Beckmann, S., Kaminski, H., Bard, D., Bau, S., Clavaguera, S., Dahmann, D., Dozol, H., Dziurowitz, N., Elihn, K., Fierz, M., Lidén, G., Meyer-Plath, A., Monz, C., Neumann, V., Pelzer, J., Simonow, B. K., Thali, P., Tuinman, I., van der Vleuten, A., Vroomen, H., and Asbach, C.: Inter-comparison of personal monitors for nanoparticles exposure at workplaces and in the environment, Science of the Total Environment, 605–606, 929 945, https://doi.org/10.1016/j.scitotenv.2017.06.041, 2017.
- Turnock, S., Butt, E., Richardson, T., Mann, G., Reddington, C., Forster, P., Haywood, J., Crippa, M., Janssens-Maenhout, G., Johnson, C., Bellouin, N., Carslaw, K., and Spracklen, D.: The impact of European legislative and technology measures to reduce air pollutants on air quality, human health and climate, Environmental Research Letters, 11, https://doi.org/10.1088/1748-9326/11/2/024010, 2016.
 - Vesisenaho, K., Kuuluvainen, H., Mäkinen, U.-V., Olin, M., and Karjalainen, P.: Data related to manuscript: Decay phase aerosol dynamics of an indoor aerosol source has a significant role in exposure analysis, Zenodo [data set], https://doi.org/10.5281/zenodo.15471503, 2025.
- Vohra, K., Vodonos, A., Schwartz, J., Marais, E. A., Sulprizio, M. P., and Mickley, L. J.: Global mortality from outdoor fine particle pollution generated by fossil fuel combustion: Results from GEOS-Chem, Environmental Research, 195, https://doi.org/10.1016/j.envres.2021.110754, 2021.
 - Wallace, L.: Indoor sources of ultrafine and accumulation mode particles: Size distributions, size-resolved concentrations, and source strengths, Aerosol Science and Technology, 40, 348 360, https://doi.org/10.1080/02786820600612250, 2006.
- Wallace, L. and Ott, W.: Personal exposure to ultrafine particles, Journal of Exposure Science and Environmental Epidemiology, 21, 20 30, https://doi.org/10.1038/jes.2009.59, 2011.
 - Wan, M.-P., Wu, C.-L., Sze To, G.-N., Chan, T.-C., and Chao, C. Y.: Ultrafine particles, and PM2.5 generated from cooking in homes, Atmospheric Environment, 45, 6141 6148, https://doi.org/10.1016/j.atmosenv.2011.08.036, 2011.
- Whitby, E. R. and McMurry, P. H.: Modal aerosol dynamics modeling, Aerosol Science and Technology, 27, 673 688, https://doi.org/10.1080/02786829708965504, 1997.
 - WHO: WHO global air quality guidelines, World Health Organization, 2021.
 - Yeung, L. and To, W.: Size distributions of the aerosols emitted from commercial cooking processes, Indoor and Built Environment, 17, 220 229, https://doi.org/10.1177/1420326X08092043, 2008.
- Yoon, H., Seo, J., Yoo, S. K., Kim, P. J., Park, J., Choe, Y., and Yang, W.: Updated general exposure factors for risk assessment in the Korean population, Journal of exposure science & environmental epidemiology, 33, 1013–1020, https://doi.org/10.1038/s41370-022-00437-6, 2022.
 - Zhao, J., Birmili, W., Hussein, T., Wehner, B., and Wiedensohler, A.: Particle number emission rates of aerosol sources in 40 German households and their contributions to ultrafine and fine particle exposure, Indoor Air, 31, 818 831, https://doi.org/10.1111/ina.12773, 2021.
- Zukowska, D., Rojas, G., Burman, E., Guyot, G., Bocanegra-Yanez, M. d. C., Laverge, J., Cao, G., and Kolarik, J.: Ventilation in low energy residences—a survey on code requirements, implementation barriers and operational challenges from seven European countries, International Journal of Ventilation, 20, 83 102, https://doi.org/10.1080/14733315.2020.1732056, 2021.